Mathematical Biosciences and Engineering

MBE, 23 (4): 813–844.
DOI: 10.3934/mbe.2026033
Received: 30 September 2025
Revised: 17 December 2025
Accepted: 23 December 2025
Published: 27 February 2026

http://www.aimspress.com/journal/MBE

*Research article*

# A deep learning and metaheuristic optimization algorithm based on Parkinson's disease classification from MRI images

**Balamurugan V[1,*] and Sivasankari K[2]**

[1] Department of Computer Science and Engineering, Akshaya College of Engineering and Technology, Kinathukadavu, Coimbatore, Tamil Nadu- 642109
[2] Department of Electronics and Communication Engineering, Akshaya College of Engineering and Technology, Kinathukadavu, Coimbatore, Tamil Nadu- 642109

[*]**Correspondence:** Email: balamuruganv@acetcbe.edu.in.

**Abstract:** Parkinson's disease (PD) is the second most common neurodegenerative disorder, characterized by the gradual deterioration of dopamine-producing neurons. The main challenge of diagnosing this disease is that physical changes in the brain begin before the patient shows outward symptoms. This leads to the necessity of developing early methods for the detection of this disease. Therefore, with the proposed model, we aimed to significantly improve the early classification of PD using MRI scans by capitalizing on advanced Artificial Intelligence (AI) and Deep Learning (DL) techniques. Our goal of the proposed model was to develop a robust medical decision-support system that enhances the diagnostic precision and supports prompt clinical intervention strategies. The method proposed was a modified EfficientNet DL model combined with the reinforcement learning optimization. This approach enabled a dynamic adjustment of model parameters to effectively minimize the misclassification rates while differentiating MRI scans of PD patients and healthy individuals. Certain performance metrics were used to calculate the performance of the proposed detection model. The results showed that the research achieved high precision, recall, and F1-score values with 98% accuracy for both classes. In the patients (class 0), the precision rate was 95%, the recall rate was 96%, and the F1-score was 98%. Similarly, for healthy individuals (class 1), the precision rate was 93%, the recall rate was 97%, and the F1-Score was 96%. Thus, the proposed EfficientNet model revealed significant enhancements in the diagnostic performance compared to the standard methods. The innovations outlined in this study emphasize the transformative power of AI in enhancing diagnostic predictions. Moreover, the convergence of a DL based EfficientNet model and reinforcement learning based metaheuristic optimization establishes a prospective implementation of

predictive analytics in managing high-risk PD with the defined objective of optimizing the patient outcomes within the field of neurology.

**Keywords:** EfficientNet; deep learning; PD; magnetic resonance imaging; artificial intelligence; reinforcement learning optimization

## 1. Introduction

In people with Parkinson's disease (PD), the motor symptoms of the body are apparent only when 60–80% of dopamine [1–3] producing cells are weakened. In addition, the number of persons with PD [4] is rising due to the world's population growth, which is placing a significant financial strain. The symptoms worsen over time due to its chronic, degenerative, and progressive nature. However, no treatment has been found to fully eradicate PD after the onset of the illness. Research has been in progress to provide patients with a better quality of life and control the gradual loss of dopaminergic neurons [5] with early identification of PD as a crucial step.

The early detection of PD can suppress the symptoms and prolong the life expectancy of PD patients. These patients' clinical diagnoses show a variety of motor and non-motor symptoms. Numerous studies have suggested that there is a higher frequency of males as PD patients than females. By 2030, there will be twice as many PD sufferers, according to particular estimates [6,7]. Moreover, magnetic resonance imaging (MRI) [8–12] can detect structural alterations in the brain caused by dopamine insufficiency in PD patients before symptoms become noticeable. The diagnosis of PD may be based on structural abnormalities in the brain. Brain MRI scan [13] analysis is the most commonly utilized diagnostic standard for the early diagnosis of PD. The anatomical information that the MRI scans reveal about the brain's subcortical structures is further examined to look for any aneurysms [14,15], which is beneficial for the early detection of an illness. However, the task becomes difficult when analyzing the key biomarkers in the studies [16–19] and complex structures of subcortical tissues from the studies [20–22]. Although ML [23–25] methods have provided good initiation to image processing, they fail when it comes to complex images such as MRI brain scans [26]. DL algorithms [27,28] have provided better results for image processing and computer vision tasks [29]. The DL model’s ability to self-learn and generalize [30] over a huge volume of data plays an important role in the automation of the decision-making process. Hence, the application of DL in classifying medical images [31] has gained a lot of interest in the research pursuit.

Correspondingly, researchers have investigated the morphological changes in the brain associated with PD, which is a relatively less explored approach. Furthermore, there has been no established system reliable for assessing the stages of PD based on imaging technology such as MRI. The study included 134 patients, categorized into test sets and training sets. The dataset included structural MRI scans [32] and evaluations based on neuropsychology. The method achieved better accuracy through the use of feature selection. An ML method was developed utilizing an SVM, and the ML method demonstrated improved and optimal efficacy in detecting the severity of PD [33].

In research, A 3D-Convolutional Neural Network (3D-CNN) architecture was created after the data was pre-processed to learn the complex patterns [34,35] in the MRI scans to detect PD. The 3D CNN [36] model outperformed the other traditional models, achieving a recall of 94.3%, a precision of 92.7%, an f1-score of 93.6%, a specificity of 94.30%, and an accuracy of 95.29%, which is better

than most methods. However, the model needs to improve the complexity of analysis to utilize a huge dataset to predict PD [37]. A Conventional method utilizes CNN [38–40] and trains it with multiple segmented brain portions. An algorithm has been introduced to amalgamate the methods from individual portions into a more complex model. The study involved a total of 305 PD patients with an average age of 59 years and 227 healthy control subjects with an average age of 61 years. The algorithm demonstrated a prediction accuracy of 94.1% when combining the fractional anisotropy from 22 regions [41].

Research indicates that PD patients often reach a dangerous stage by the time they are diagnosed. To facilitate early diagnosis, new methods are continually being explored by researchers. A conventional study suggests using DL methods to diagnose PD and multiple system atrophy and to distinguish healthy individuals. The data for the conventional study was sourced from Istanbul University Cerrahpasa Faculty of Medicine Hospital. The original MRI scan processing was supervised by the doctors from the sourcing hospital. Conventional research has been aimed at enhancing the neural network to achieve better results in image analysis and disease detection. Although the system is suitable for the detection of characteristics associated with PD, it needs improvement in the augmentation of large datasets and the precision of classification. However, important indicators such as accuracy and performance metrics should be improved [42].

### *1.1. Motivation*

PD drastically affects the quality of people, especially in middle and older age, at which the health of an individual is very important. The manifestation of PD increases with time almost irreversibly and cannot be cured. However, early detection can mitigate the effects of PD and prolong the life expectancy of PD patients to a considerable extent. For the prior detection of PD, MRI is the most preferred tool, which can image the most complex structures of the brain. The morphological changes of the brain occur before symptoms. However, the availability of skilled professionals, time, and cost is very limited. Hence, many researchers turn to use Artificial Intelligence, particularly DL models, for the classification of normal and PD patients with MRI scans. However, the conventional system often fails to provide adequate accuracy and overall reliability in PD detection. Thus, the proposed model uses Deep Learning and Metaheuristic Optimization Algorithms to classify the MRI scans into PD-affected cases and normal individual scans. The PPMI dataset is utilized in this study to train and test the proposed system. The Modified EfficientNet with Feature Sculptor Spatial Net by Crafting Precision through Layers algorithm is utilized for the classification process, which results in better performance. Additionally, the Reinforced Learning Optimization Algorithm for feature Optimization enhances the accuracy of the proposed system. The proposed system provides better performance in the binary classification of PD.

### *1.2. Research contribution*

- To perform feature extraction using CNN for extracting relevant features required for the proposed model.
- To implement the proposed feature optimization using a deep reinforcement learning approach to continuously modify characteristics according to input received for enhancing the performance of the model.

- To perform binary classification of PD using the proposed EfficientNet layer, where Feature Sculptor Spatial Net is used to classify the healthy individuals from Parkinson patients.
- To assess the performance of the proposed framework using metrics such as accuracy, recall, precision, and F1 score.

The structure of the article is organized as follows to effectively project the proposed PD classification: In Section II, we present an analysis of traditional research in the field. The methodology implemented in the proposed research is outlined in Section III. Following this, in Section IV, we illustrate the results achieved by the respective model. We conclude the paper in Section V, which discusses the conclusion and future work of the proposed method.

## 2. Literature review

PD is a neurodegenerative condition that mostly affects the elderly population. PD is characterized by the progressive degeneration of dopaminergic neurons present in the substantia nigra pars compacta. As the disease progresses, patients experience mobility issues such as tremors, slow movement, and problems with balance and posture. These symptoms gradually increase over time. The most effective way to manage PD is through early detection. However, the prior identification process is often limited by a shortage of skilled professionals. Moreover, the rapid advancements in AI and ML technologies [43,44] have enabled automatic image analysis, but often lack complexity in the algorithms to handle complicated data, such as MRI scans, and are limited by scalability. They are particularly well-suited for handling complex decision-making tasks, especially in the field of image classification [45]. Moreover, this study has highlighted the need to integrate some advanced ML methods that can surpass the complexity and variability of the clinical MRI scans to enhance the accuracy of diagnostics and clinical implementation. It has been also insisted to improve the medical imaging algorithms to ensure their application in the real-world clinical structures [46]. In research, efforts have been made to categorize MRI images of healthy individuals and those with PD utilizing a DL neural network. The CNN architecture, AlexNet [47,48], is employed to enhance the diagnosis of PD. The MR images are trained using a transfer learning [49,50] network and tested to determine accuracy measures. This system has achieved an accuracy rate of 88.9%. Additionally, Dl models have the potential to assist medical professionals in diagnosing PD. However, the system should provide a more objective and improved classification of PD [51]. In research, two innovative approaches utilizing DL methods have been employed, such as 2D and 3D CNN trained on MRI scans in the axial plane. The dataset has been assembled using images from the PPMI, with a total of 318 MRI scans used for training and testing 2D [52,53] and 3D CNN models. The 3D model has been successful in learning crucial features from the data and managed to classify the test data with an accuracy of 88.9%. On the other hand, the 2D model achieved an accuracy of 72.22%, which indicates that there is a need to improve the accuracy of the targeted research problem [54].

Similarly, it has been stated that the diagnosis and segmentation of the brain tumors and other neuro diseases start with a non-invasive imaging technique known as MRI. As there is a need for human intervention, there is an increased risk of diagnostic misinterpretation. Thus, developing robust automated neuro disease detection techniques has been widely considered over the past years [55]. The research explores the potential of ML in diagnosing PD, with a focus on identifying the non-motor symptoms that manifest early in the disease's progression. The existing system aims to detect the symptoms at the initial stages to prevent the disease from advancing. For the classification of PD, the

method utilized Classification and Regression Trees, ANN [56], and SVM [57,58] in the experiments. However, the system needs to improve in the complexity of data processing and feature optimization [59]. Determining the levels of PD and predicting its development is a crucial process. Moreover, the application of supervised and unsupervised AI and ML techniques to clinical datasets to classify image data is utilized in the research. The approach aimed to accurately diagnose PD, identifying its stage, and predicting its course. The results indicated that the CNN model based on MRI could serve as an effective method for differentiating PD levels with a considerable accuracy of 0.94. However, the system lacks diversity in the of datasets and performance metrics [60]. Moreover, the results of the study outlined the effectiveness of MVO-based CNN VGG16 and ResNet50 models for the classification of brain tumors from the MRI images. In the future, the examinations could include the applicability of DL models in addressing the multiclass issues and the clinical limitations [61]. Correspondingly, the study has dealt with a smaller part of the brain image with a simple and efficient Cascade Convolutional Neural Network (C-ConvNet/C-CNN) technique. This CNN-based model has enhanced local and global features of the method [62].

Research presents two DL-based frameworks, namely feature-level and modal-level, designed to classify subjects into PD and healthy categories. These classifications are based on MRI scans that are T1 weighted, SPECT, and CSF-featured datasets. The formation of the heterogeneous dataset for the feature-level framework differs from that of the modal-level framework, even though both datasets comprise neuroimaging and biological markers [63]. The feature-level framework, using CNN, achieved a maximum accuracy of 93.33%. In contrast, the modal-level framework recorded an accuracy of 92.38%. The system needs to improve in overall accuracy and other performance metrics [64]. The importance of textural and morphological analysis is substantial as it enables the quantification of grey-level patterns and the establishment of relationships between pixels within specific regions of interest. Three unique gait datasets, which include VGRF collection for various walking scenarios, are utilized to train the LSTM [65] network. To prevent overfitting [66] of data, the system incorporates L2 regularization and dropout methods. However, the system needs to improve in the image preprocessing and extraction to avoid the impact of noisy data on the results [67]. Eventually, the considered study has utilized a CNN-based model for exploring the descriptions from the brain tissue from the four input patches. Overall, the method has outperformed the classical methods with the dice score and recall [68].

Correspondingly, the effectiveness of the method MGWO-eP is examined by the benchmark optimization function in order to reach the global optimum. Following this, the model has achieved overall accuracies of 96.30% (with voting), 94.45% (with random forest), and 98.31% (with voting) by surpassing the GWO and PSA models [69]. Additionally, the researchers have identified the biomarkers using these techniques by offering some perceptions for improving the diagnostic process. The discussion has included different data formats of ML and DL methods in the diagnosis of PD [70]. Accordingly, a comparative analysis was performed by the model for measuring the effectiveness of the dual-target stimulation with respect to the single-target stimulation. The dual-target stimulation method has demonstrated approximately 83% accuracy in the tremor amplitude and 76% accuracy in the produced electrical field intensity (EFi) [71].

There is a method that utilizes deep convolutional neural networks to categorize MR images of healthy individuals and those diagnosed with PD. The approach implements a DCNN classifier that integrates data augmentation and transfer learning methods to enhance the classification process. The dataset is a collection of 504 images, of which 360 images have been used for data augmentation. The

results indicate that fine-tuning the final layers provides 89.23% accuracy [72]. Likewise, in the study, the utilized pretrained YOLOv8-L model achieved 0.269 IoU by sustaining classic object detection models such as Mask R-CNN and Faster R-CNN [73]. The performance of SVM, RF, KNN, and Logistic Regression models has been compared for classification results. The RF classifier developed as the optimal machine-learning technique for PD detection. The model demonstrated an accuracy of 91.83% and a sensitivity rate of 0.95 [74].

Sequentially, the study has presented a framework that utilizes blockchain technology for improving the segmentation in medical imaging. The researchers addressed the issues related to data security, such as data privacy, annotation accuracy, and collaboration [75]. The dataset size utilized in neuroimaging studies for Alzheimer's disease varies by limiting the generalizability of findings due to small sample sizes and diverse participant characteristics [76]. The analysis included 59 FDA-cleared AI algorithms for neuroimaging; however, the generalizability of these findings may be limited due to the lack of clinical validation confirming the advertised value propositions in real-world practice [77–79]. The paper highlights AI applications in multiple sclerosis but does not specify dataset sizes; thus, the generalizability of the findings may be limited due to a lack of clinical validation and the need for improved model interpretability and transparency [80–83].

**Research gap**

| REF | AIM/OBJECTIVE | METHODOLOGY | APPLICATIONS | LIMITATIONS |
|---|---|---|---|---|
| [46] | To compare BraTS with real clinical dataset features. | Comparative data analysis. | Has highlighted the challenges of clinical data diversity. | Limited accuracy due to selection bias |
| [61] | To develop a high-accuracy MRI classification method. | Optimized combined VGG16 and ResNet50 models with MVO. | Has classified MRI images as tumor or non-tumor. | Prone to overfitting on specific datasets |
| [62] | To develop a fast and effective brain tumor segmentation system. | Partial pre-processing, C-CNN model, and Distance-Wise Attention. | Has reduced the computation time and improved segmentation accuracy. | Vulnerable to the variability of input data |
| [73] | To examine the pretraining impact on YOLOv8 model performance. | Pretrained vs. non-pretrained YOLOv8 models. | Has improved tumor localization model's accuracy via pretraining. | Required quality data and high computational power |
| [75] | To improve tumor segmentation and clinical data security | Blockchain and smart contracts | Cancer diagnosis, treatment planning, and medical AI development | High computational demands and dependent on specific data protocols |

*2.1. Problem identification*

- The performance of a model is often assessed by its accuracy, which is an important metric. Although numerous researchers have aimed to achieve efficient PD classification, they often fall short in terms of the accuracy metric [51,54,72].
- The conventional model employed a framework based on CNN for PD classification, using neuropsychological and MRI images but was limited by the complexity of the data [38–40].
- Several research methods using DL algorithms to detect PD lack a diversity dataset used for training and the preprocessing methods to enhance the performance and optimize the training time [59,60].

## 3. Proposed methodology

PD can vary widely from person to person, and it is challenging to provide the ranking of severity across the world. It is necessary to detect disease earlier to avoid future consequences. The identification of PD without using advanced models can be a time-consuming process and can be prone to human error. To tackle the issue, traditional researchers have utilized AI-based technology for the automation of PD classification. However, classical systems face some challenges like accuracy, over-fitting of data, and scalability. To resolve the issue, the proposed model utilizes a particular procedure for PD classification. Figure 1 signifies the design flow of the proposed model.

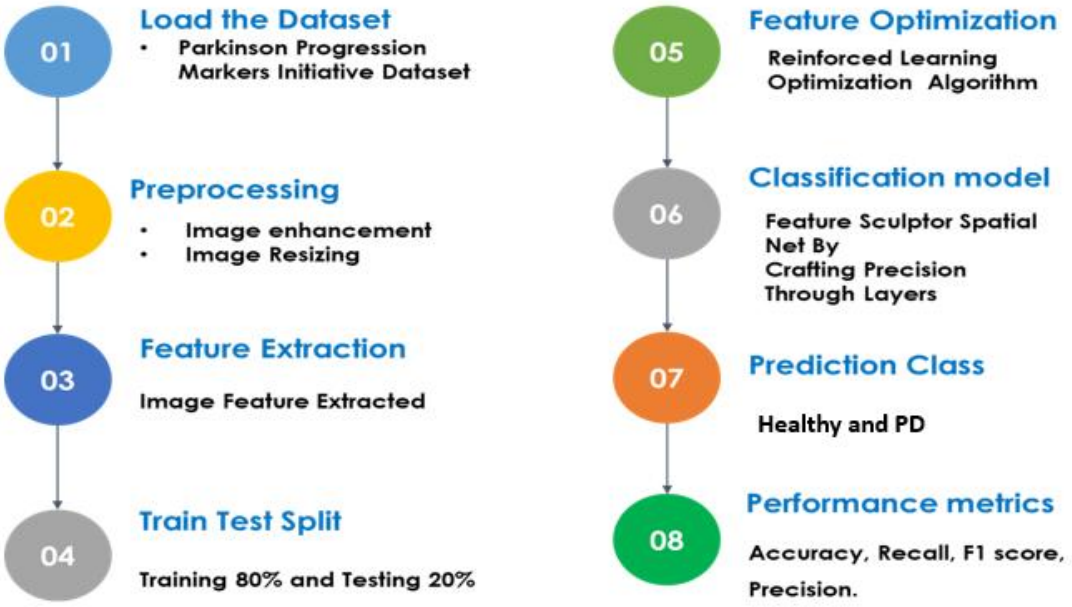


**Figure 1.** Design Flow of the Proposed Model.

Figure 1 is the simplified workflow of the proposed PD classification system. The diagram illustrates the three-stage pipeline such as MRI preprocessing, Feature Sculptor Spatial Net (FSSN) with Reinforcement Learning Optimization Algorithm (RLOA), and binary classification. This streamlines the integration of DL and reinforcement learning for accurate PD detection.

### *3.1. Pre-processing*

Pre-processing is used in the proposed system using the Feature Sculptor Spatial Net Layers for classifying the healthy individuals and those with PD with the Parkinson's images to prepare the dataset for the classification. Here, two types of pre-processing techniques are used: image enhancement and image resizing. In this structure, two subcategories of the pre-processing techniques are utilized for improving image quality and adjusting image size. These methods are essential for enhancing the quality and structure of the images as well as for guaranteeing ideal input for future classification algorithms. Enhancement of the images is important for the classification, whereas resizing the images can ensure consistent dimensions. Precise pre-processing procedures are important for improving the model's capability to classify Healthy and PD categories of PD images.

#### 3.1.1. Image enhancement

The image enhancement process involves several steps for optimizing the input images for more an accurate feature extraction. At first, the contrast stretching is applied for adjusting the image intensity levels, which increases the difference between the foreground and background. Then, sharpening techniques are used to highlight the edges by emphasizing high-frequency components of the image. Noise reduction algorithms, such as Gaussian filters or median filtering, are employed to reduce unwanted noise and artefacts. Histogram equalization is performed to adjust the image's pixel intensity distribution for improving the contrast and visual clarity. These enhancements result in a clearer and a distinguishable image in order to allow the EfficientNet model to focus on critical features during the classification process. The combination of these techniques ensures that the network processes high-quality images by maximizing the model's accuracy and efficiency.

#### 3.1.2. Image resizing

In the proposed method, the image resizing process involves a series of steps designed to optimize feature extraction and improve model performance. Initially, the original image is captured or loaded into the system. To maintain visual consistency, the aspect ratio of the image is preserved during the resizing by preventing any distortion in the spatial features. The image is then resized to a target size of 300x300 pixels using interpolation methods such as bilinear or bicubic interpolation. Following this, the pixel values are normalized, typically scaled between 0 and 1 based on the dataset's mean and standard deviation. To enhance dataset diversity and model robustness, the data augmentation techniques are applied. If necessary, RGB images are converted to grayscale. Finally, the resized and processed image is transformed into feature maps that are compatible with the EfficientNet architecture.

### *3.2. Feature extraction*

Feature extraction is employed using Convolutional Neural Networks. Though there are various models, the proposed model uses CNN for feature extraction because, CNN-based feature extraction can eliminate the errors. Convolutional Neural Networks play a crucial role in the PD classification process due to their ability to process complex data and identify relevant patterns effectively. CNNs are designed to automatically extract the hierarchical features from the input data, by applying convolutional filters and pooling operations across multiple layers. These extracted features represent

essential characteristics of the data for enabling the model to distinguish healthy individuals and Parkinson's patients. In CNNs, the convolutional layers are applied to detect the spatial patterns, that reduce dimensionality while preserving critical information. As the network deepens, it captures the abstract features, which are pivotal for accurate classification.

### *3.3. Data splitting*

Data splitting involves dividing the dataset into training and testing subsets to evaluate the classification model's effectiveness with the new data. The ratio is set at 80:20, with 80% for training and 20% for testing. This proportion helps the model to learn from various examples during the training and assess its ability to generalize to unseen data during testing. The training data is used to teach the Feature Sculptor Spatial Net to detect important characteristics from input images and to reduce the prediction errors. The model's performance is evaluated with testing data, particularly in classifying the PD images. Proper data splitting is vital to prevent the over-fitting and ensure the model's accuracy with new data. Using an independent testing dataset helps researchers to gain reliable evaluation of the model's actual performance.

### *3.4. Feature optimization: Reinforced learning optimization algorithm*

In the described system, the Reinforced Learning Optimization Algorithm (RLOA) for feature optimization follows a series of important steps in the working process. In the system mentioned, feature optimization involves the improved features extracted by the CNN to enhance classification performance. This process includes using a RLOA to continuously modify the characteristics according to the input received. Reinforcement learning principles help the algorithm maximize the cumulative reward by modifying the parameters of the Feature Sculptor Spatial Net to enhance its efficiency. Figure. 2 signifies the feature optimization method of the proposed system.

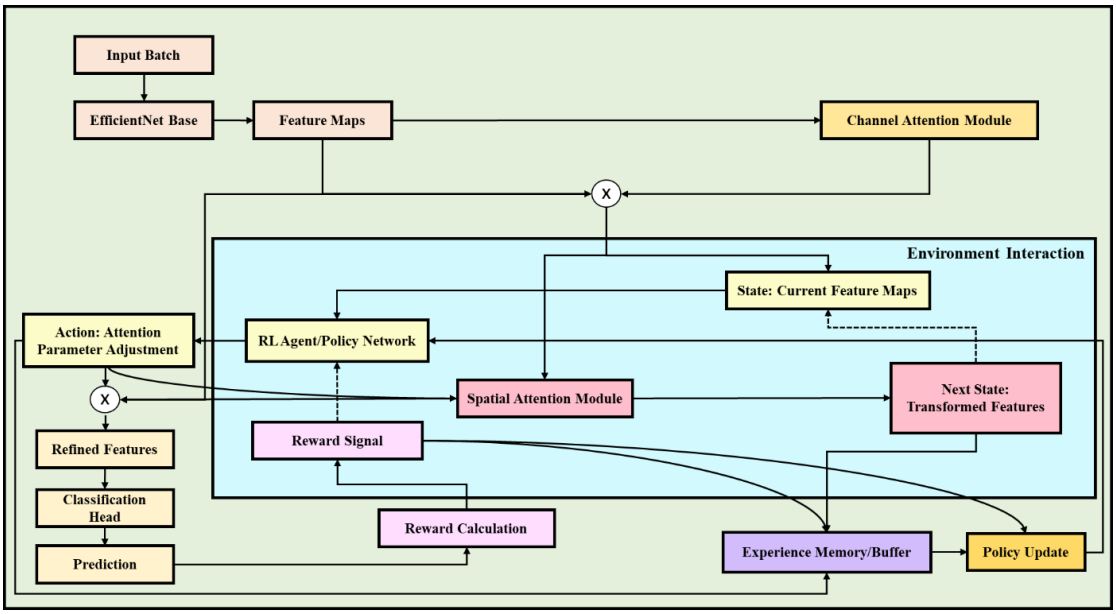


**Figure 2.** Reinforced Learning Optimization Algorithm.

Figure 2 shows how the RL agent dynamically adjusts the attention parameters in the Feature Sculptor Spatial Net (FSSN) using reward feedback. This adaptive mechanism optimizes discriminative features for PD classification, directly addressing limitations of static feature extraction in prior work.

The RL agents select the actions for modifying the attention parameters, assisted by a reward system, which assesses the performance of alterations. The above feedback loop permits continuous learning via reward calculation and policy updates, enhancing the decision-making of the agent after a certain time. Also, the experience memory saves the earlier interactions to increase the learning effectiveness. The refined features are further transferred to the classification head, providing the final forecasting. Hence, the dynamic environment interaction raises the effective training, with an RL agent, unconventionally optimizing attention mechanisms. The fusion of spatial and CAM enables the précised feature refinement, whereas the policy network assures adaptive learning without manual interpolation. Eventually, the RL results in enhanced classification performance, as the model iteratively adapts for more robust and generalized feature representations. Therefore, the process is described as follows:

- Input Batch: The process starts with an Input Batch, which is fed into the EfficientNet Base.
- EfficientNet Base: The EfficientNet Base processes the input and generates Feature Maps. EfficientNet-B3 is a network model with unique features whose design benefits from the experience of other good neural networks.
- Feature Maps: The generated Feature Maps are then passed to a CAM.
- Channel Attention Module (CAM): The CAM assigns weights to the feature maps of each channel to improve the response of important channels.
- Environment Interaction: The feature maps from EfficientNet Base also enter the "Environment Interaction" block, which is central to the reinforcement learning aspect of the system. The current State is defined as the "Current Feature Maps".
- RL Agent/Policy Network: An RL Agent/Policy Network interacts with the environment.
- Spatial Attention Module (SAM): The SAM assigns weights to the feature maps of each spatial location to improve the response of important locations.
- Next State: The output of the SAM is the Next State, which is labelled as "Transformed Features".
- Reward Signal: A Reward Signal is generated based on the transformation.
- Reward Calculation: The reward Calculation block is connected to the Next State and feeds into the Reward Signal.
- Action: Attention Parameter Adjustment: The RL agent takes an Action to adjust the attention parameters. This action influences the Spatial Attention Module and, through multiplication with the output of the Channel Attention Module, refines the features.
- Refined Features: The refined features are then passed to a Classification Head.
- Classification Head: The Classification Head processes the refined features to produce a Prediction.
- Policy Update: The Experience Memory/Buffer stores the experiences, and the Policy Update block uses these experiences to update the RL agent's policy.

Therefore, the integration of the DRL process in feature optimizations aids in better performance of the model, which can also assist in an effective classification mechanism.

*3.5 Classification mechanism*

The method "Feature Sculptor Spatial Net by Crafting Precision through Layers" is an advanced technique for categorizing PD into groups like Healthy and PD within a CNN structure. It involves a diverse approach that includes extracting features by analyzing the spatial data, and designing the layers with the precision. The idea of "Feature Sculptor" highlights the importance of identifying and molding the relevant characteristics found in the medical images related to the PD, such as complex designs and surface qualities. The addition of "Spatial Net" indicates the integration of spatial processing layers, such as convolutional layers for capturing the spatial relationships in the images. This allows the model to differentiate the spatial distributions of important features. Furthermore, by focusing on "Crafting Precision through Layers," the approach guarantees a careful planning and fine-tuning of network layers in the classification. The thorough incorporation of these elements is focused on obtaining precise and dependable classification outcomes, leading to enhanced diagnosis and treatment of PD. By utilizing advanced CNN architecture and precision-focused techniques, the methodology tackles the intricacies of PD classification to improve diagnostic capabilities and benefit patient outcomes.

3.5.1. Traditional EfficientNet

In 2019, Google researchers created EfficientNet, a revolutionary Convolutional Neural Network architecture tailored to enhance the trade-off between computational efficiency and model performance for image classification tasks. It provides unique benefits for a range of uses by increasing the network's depth, width, and resolution. By utilizing its ability to scale and perform well, the EfficientNet offers a potential way to effectively classify medical images like "healthy" and "PD". The architecture of the classical EfficientNet is mentioned in Figure 3.

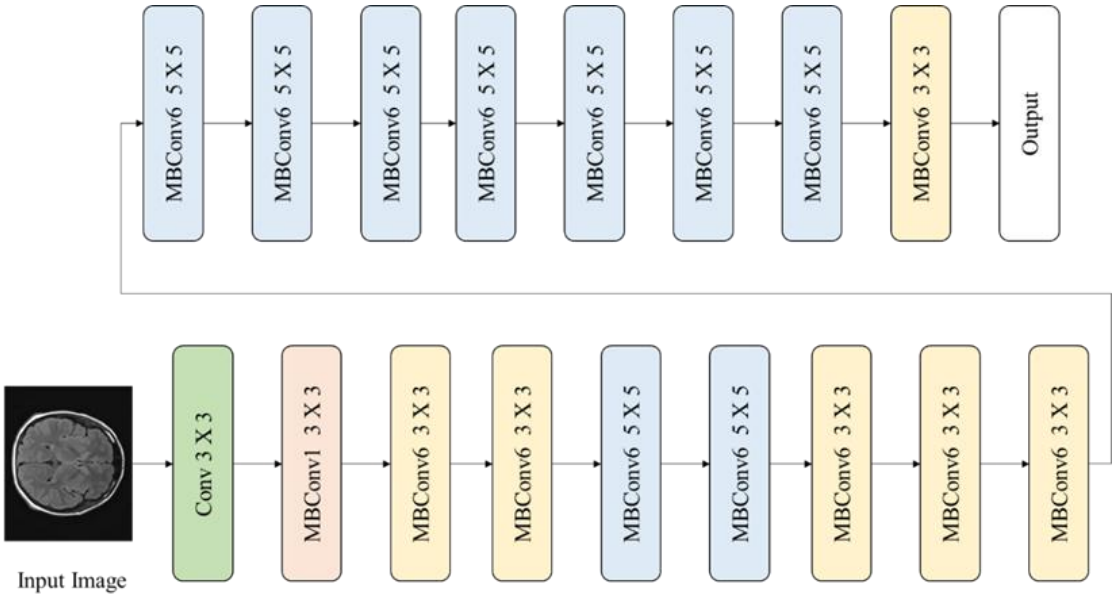


**Figure 3.** Architecture of the Conventional Efficient Net.

Figure 3 depicts the traditional efficient net architecture when applied to the Parkinson's Images Dataset into Healthy and PD groups. This is followed by the structured sequence for the feature extraction and manipulation. The process begins with the Parkinson's Images Dataset, containing the input images that depict various presentations of the PD. The first layer applies a 3×3 convolution (Conv 3×3) to the detect fundamental features like edges and textures. This is followed by the MBConv1 3×3, by representing a MobileNetV2 inverted bottleneck convolution with a 1x expansion factor for performing depth-wise separable convolution and point-wise convolution to capture basic features. The network then utilizes MBConv6 3×3for enhancing the feature representation with the depth-wise separable convolutions and point-wise convolutions. This is repeated with another MBConv6 3×3, for further enriching the feature extraction. The model incorporates MBConv6 5×5, using a larger 5×5 kernel to capture broader spatial patterns, followed by additional layers with the same 5×5 kernel to deepen the spatial feature extraction. The process continues with the multiple MBConv6 3×3 layers to refine and extract the detailed features using the MBConv6 5×5 layers to maintain spatial context. This iterative feature extraction strategy can ensure the comprehensive learning of complex patterns associated with the PD. The final layer aggregates the refined features to produce the classification outputs in order to provide the predicted labels or probabilities for each image to categorize them as Healthy and PD.

**Algorithm. I. Existing EfficientNet**

Input : PPMI Dataset $\{a_1, a_2, \ldots a_z\}, q = 1.0, w = 1.1$
Output : Classification $\{c_1, c_2, \ldots c_z\}$
for each image $\{a_1, a_2, \ldots a_z\}$ do
ppmi dataimage = image ( ppmi);
$layer_{32} = convlayer3(ppmi\ dataimage)$
$layer_{16} = MBconv1layer3(layer_{32})$
$layer_{24} = MBconv6layer3(layer_{16})$
$layer_{40} = MBconv6layer5(layer_{24})$
$layer_{80} = MBconv6layer3(layer_{40})$
$layer_{112} = MBconv6layer5(layer_{80})$
$layer_{192} = MBconv6layer5(layer_{112})$
$layer_{320} = MBconv6layer3(layer_{192})$
$layer1_{320} = convlayer1(layer_{320})$
$layer2_{320} = Pooling(layer1_{320})$
$layer_{1280} = FClayer(layer2_{320})$
$layer1_{1280} = GlobalavgPoolinglayer(\ layer_{1280})$
$c_1, c_2, \ldots c_9 = softmax(layer1_{1280})$
end

Commonly, the Efficient Net structure enables efficient and successful extraction of features, which helps its performance in classifying PD using medical images. Efficient Net provides multiple important benefits that make it a strong option for classifying PD. First, by optimizing the trade-off between performance and computational efficiency, it achieves high accuracy with minimal

computational resources. This effectiveness is especially advantageous in medical fields, where there may be a high presence of computational limitations. Moreover, Efficient Net's ability to scale enables it to be easily tailored to different kinds of hardware, guaranteeing flexibility when being used in various settings. Furthermore, its proven exceptional performance in standard image classification challenges, particularly in medical datasets, highlights its ability to accurately identify PD using medical images.

Although EfficientNet has multiple benefits, it comes with some restrictions and difficulties. Significant computational resources may be needed for training and fine-tuning due to the inherent complexity, particularly when working with large datasets or complicated classification tasks. Furthermore, understanding the internal representations acquired by EfficientNet may present difficulties, potentially impeding our comprehension of how it makes decisions. The potential restriction in medical applications due to a lack of interpretability may limit its usefulness in domains where transparency is important.

### 3.5.2. Proposed EfficientNet System: Feature sculptor spatial net by crafting precision through layers

The traditional EfficientNet models, while efficient, face limitations such as reduced adaptability to complex datasets and insufficient feature refinement capabilities. Their fixed scaling approach often struggles to capture intricate spatial relationships and detailed patterns. Thus, the proposed Feature Sculptor Spatial Net enhances EfficientNet by integrating dynamic spatial attention mechanisms for precise feature extraction. This model enables adaptive focus on significant image regions, improving accuracy and robustness, especially for complex image classification tasks. The advantages of the Proposed EfficientNet include enhanced feature refinement, dynamic spatial attention for adaptive learning, superior accuracy in complex datasets, efficient scalability, and reduced overfitting, making it more reliable and effective compared to traditional models.

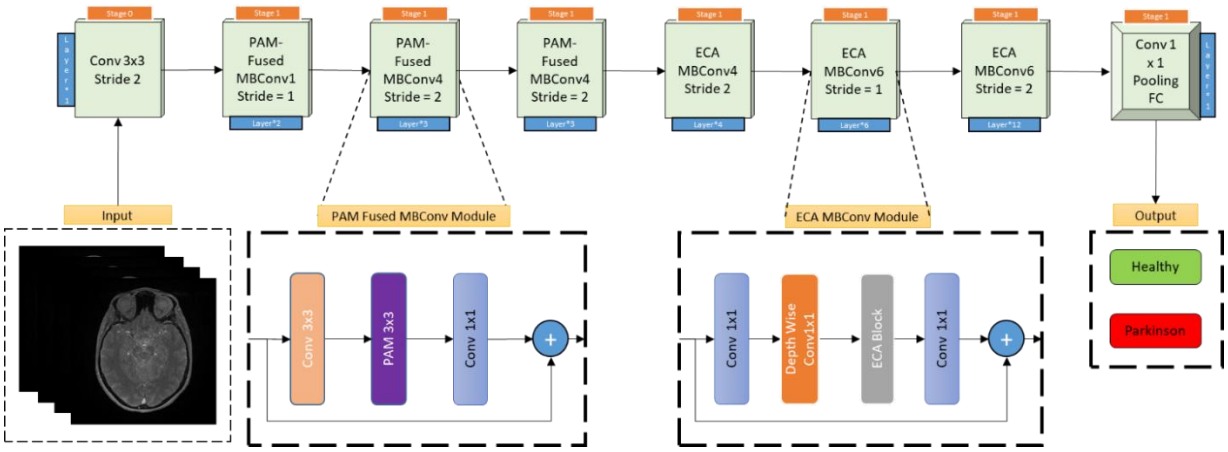


**Figure 4.** Architecture of the Proposed Efficient Net.

Figure 4 depicts the proposed efficient net for brain MRI scan classification begins with the input Layer, where a pre-processed grayscale MRI scan is fed into the network. These pre-processing steps include skull stripping, bias field correction, and intensity normalization to standardize the images, ensuring consistency and enhancing the model's performance. The process progresses to Stage 0

(Initial Feature Extraction), where a 3×3 Convolutional Layer with a Stride of 2 acts as the primary feature extractor. This layer captures local patterns such as edges and textures while reducing the image's spatial dimensions, thus decreasing computational complexity and expanding the receptive field for subsequent layers. In Stage 1 (Feature Refinement and Attention), the model incorporates PAM-Fused MBConv Modules for early feature refinement. The Positional Attention Module (PAM) calculates spatial attention weights, emphasizing diagnostically relevant regions within the MRI scan, which is followed by MBConv, which utilizes depth-wise separable convolutions and an inverted residual structure to enhance efficiency. These modules, supported by batch normalization and activation functions like ReLU or Swish, help in learning robust features. The stride varies across these modules starting with stride 1 to preserve spatial resolution for fine details and transitioning to stride 2 for down-sampling in deeper layers.

As the model progresses, ECA MBConv Modules further refine the features by introducing Efficient Channel Attention (ECA). This mechanism assigns importance to informative channels while suppressing less relevant ones, improving the representational capacity without significant computational overhead compared to other attention mechanisms like SE blocks. The consistent use of MBConv structures with residual connections ensures efficient learning throughout the network. Hierarchical feature learning is achieved through the repetition of these modules, capturing low-level details (edges, textures) and high-level patterns. The architecture then moves to the Final Layers, where a 1x1 Convolutional Layer reduces dimensionality. This prepares the data for the Fully Connected (FC) Layer, which performs the final classification. A SoftMax activation function generates probability scores for the two output classes: Healthy and Parkinson's. The Output Layer produces two probability scores, indicating the likelihood of the MRI scan belonging to each class. The class with the higher probability is chosen as the predicted diagnosis. The network is trained on labeled datasets of brain MRIs from healthy individuals and Parkinson's patients, utilizing binary cross-entropy loss functions. Equation 1 shows the application of the attention mechanism N(G) to the input feature map G, resulting in an enhanced feature map G'. Furthermore, Equation 2 applies a second attention mechanism N(G') to the previously enhanced feature map G' for further refinement.

$$G' = N_c(G) \otimes G_1 \tag{1}$$

$$G'' = N_s(G') \otimes G' \tag{2}$$

The input feature map, denoted as $G$, is processed through various attention mechanisms to enhance feature representations. The mathematical term of ECA is given below in equations 3 and 4. Equation 3 defines the ECA (Efficient Channel Attention) mechanism, combining average and max-pooled features processed through MLPs to generate channel attention weights, whereas equation 4 has given an alternative definition of ECA using bottleneck structures to refine the average and max-pooled features by outputting attention weights.

$$N_c(\boldsymbol{G}) = \sigma\left(MLP\left(AvgPool(\boldsymbol{G})\right) + MLP\left(MaxPool(\boldsymbol{G})\right)\right) \tag{3}$$

where $AvgPool(\boldsymbol{G})$ and $\left(MaxPool(\boldsymbol{G})\right)$ denote the average and max pooling operations to the feature map $G$, respectively, capturing global and dominant features. $MLP$ denotes the Multilayer Perceptron for processing the pooled features through fully connected layers to learn complex relationships.

$$N_c(\boldsymbol{G}) = \sigma(B_1(B_0(\mathrm{G}^c_{\mathrm{avg}})) + B_1(B_0(\mathrm{G}^c_{\mathrm{max}})) \tag{4}$$

where $B_1, B_0$ denote the bottleneck structures or additional layers to further refine features, and $\sigma$ outputs the attention weights, emphasizing important channels and suppressing irrelevant ones.

The mathematical term of Spatial Attention Mechanism (SAM) is given below in equations 5 and 6. Equation 5 defines the SAM, concatenating average and max-pooled features and applying a 7x7 convolution to generate spatial attention weights.

$$N_s(\boldsymbol{G}) = \sigma(f^{7\times7}([AvgPool(\boldsymbol{G}); MLP(MaxPool(\boldsymbol{G})])) \tag{5}$$

where $AvgPool(\boldsymbol{G})$ and $MaxPool(\boldsymbol{G})$ denote the average and max pooling across spatial dimensions to capture global and local spatial information, and $f^{7\times7}$ denotes a convolutional operation with a 7×7 kernel to model spatial dependencies effectively. Equation 6 illustrates the concatenating average and max pooled features across spatial dimensions, applying a 7x7 convolution.

$$Ns(\boldsymbol{G}) = \sigma(f^{7\times7}([\mathrm{G}^s_{\mathrm{avg}}; \mathrm{G}^s_{\mathrm{max}}])) \tag{6}$$

where $\sigma$ is the sigmoid activation which produces spatial attention maps and $Concatenation$ ([ ]) combines the pooled features to provide a spatial context. The feature refinement steps are given in equations 7 and 8,

$$G_2 \quad = N_c(G_1) \otimes G_1 \tag{7}$$

$$G_3 = N_s(G_2) \otimes G_2 \tag{8}$$

Equation 7 improves the feature map $G1$ to produce an enriched feature map $G2$. Further, equation 8 improves the spatial attention to focus on creating the critical spatial regions $G3$, where $\otimes$ signifies the element-wise multiplication that applies the attention masks to the feature maps and $G_1, and\ G_2$ represent progressively refined feature maps through successive applications of ECA and SAM.

Therefore, the proposed EfficientNet model with Feature Sculptor Spatial Net offers several advantages. First, it enhances model precision by crafting features through multiple layers. Second, the system uses the EfficientNet's architecture, which optimizes accuracy and computational efficiency. Last, the proposed model used for the classification approach enables superior performance in tasks involving complex data, making it highly effective for the detection of PD.

## 4. Results & discussion

This section represents the outcome accomplished by the proposed model. We provide an overview of the input data and performance metrics used to examine the projected system's efficiency. Additionally, we provide the experimental results and analyze the efficiency of this study. Moreover, we compared the proposed model with the traditional algorithms for explaining the greater efficiency of the proposed approach.

### *4.1. Dataset description*

The Parkinson's Progression Markers Initiative (PPMI) dataset is utilized by the proposed model

for PD detection. PPMI enables researching the disease progression, biomarkers, and treatments by gathering the data from the individuals with PD, those at risk, and healthy controls. This diverse dataset includes different types of data, such as clinical evaluations, imaging tests, genetic data, biospecimen samples, and demographic information. The longitudinal structure of PPMI enables tracking disease progression and treatment effects by collecting data at various time points over multiple years. The dataset is available to eligible researchers, promoting teamwork and speeding up advancements in PD research while following ethical and data-sharing rules. Correspondingly, the proposed method uses the structural MRI scans for the classification of PD as Healthy and PD. We utilize a total of 25,000 images for the training process. The training set is perfectly balanced with 12,500 images for the Healthy class and 12,500 images for the PD class. For the testing phase, an independent set of 8,980 images is used, consisting of 4,706 Healthy images and 4,274 PD images. The counts are derived directly from the confusion matrices provided in Figure 12. Dataset availability: https://www.ppmi-info.org/access-data-specimens/download-data/. Further, all patient data is de-identified with prior informed consent, adhering to the PPMI's ethical guidelines.

### *4.2. Exploratory Data Analysis (EDA)*

The EDA is used to view and analyze the data in the Parkinson's Images Dataset. Figure 5 represents the data from the PPMI dataset that indicates the class “healthy”.

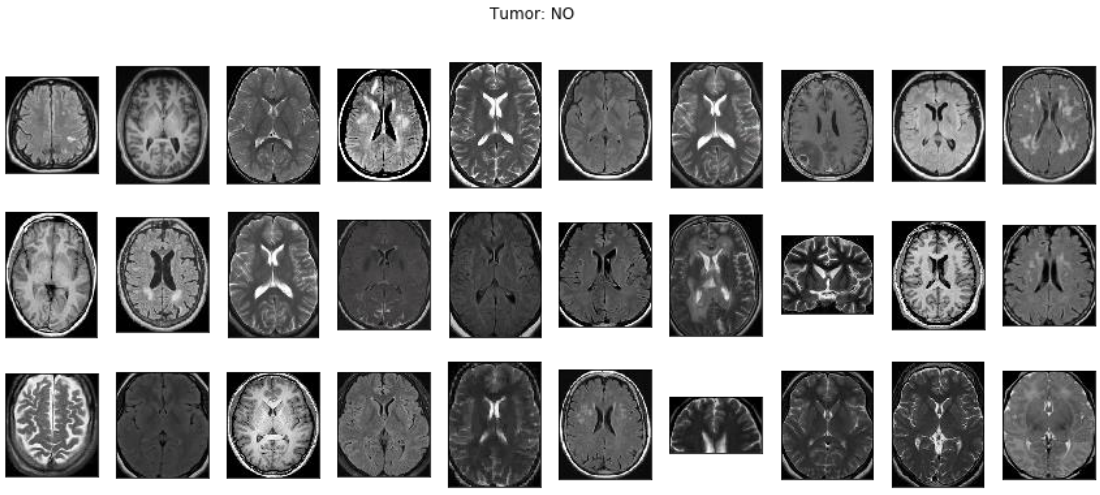


**Figure 5.** Class-Healthy data from Parkinson’s Images Dataset.

Figure 5 depicts a portion of data taken from the Parkinson's Images Dataset. This dataset consists of the medical images utilized for the examination and identification of PD. The data split ratio utilized by the proposed model is 80% for training and 20% for testing. In this representation, the prominence is on the occurrences that are classified within the category marked as "healthy”. In the dataset, "healthy" indicates the instances where people show no signs of PD or any associated issues. These pictures are important for comparing and analyzing the differences or irregularities linked to PD. Through an examination and analysis of the data shown in Figure 6, the researchers and healthcare professionals obtain an understanding of the attributes and elements found in typical cases within the

dataset. This knowledge is essential for creating the diagnostic tools and for progressing the research for the means of early detection and intervention of PD.

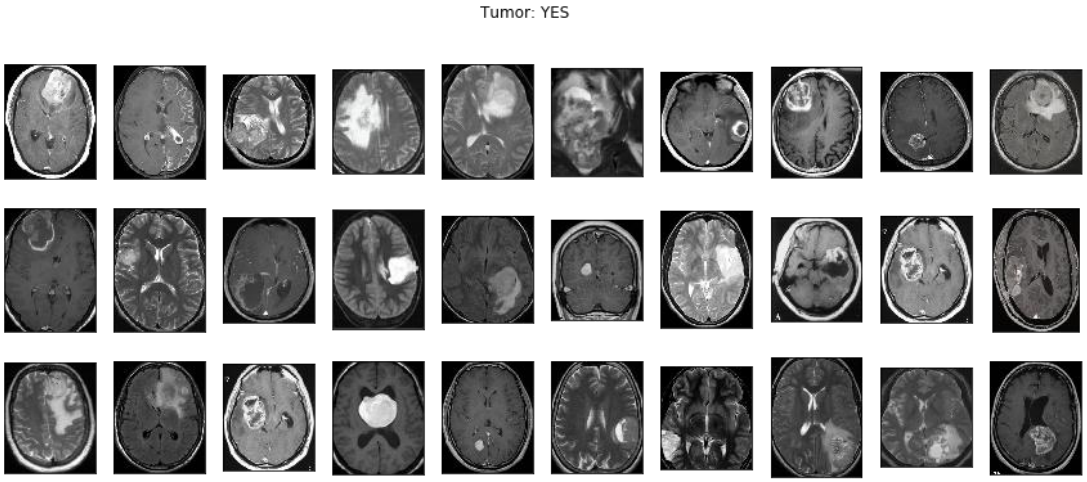


**Figure 6.** Class-PD data from the Parkinson's Images Dataset.

Figure 6 indicates the class "PD" from the Parkinson's Image Dataset. Within the Parkinson's image dataset, the category "PD" indicates the occurrences of unusual growths or masses identified in medical imaging.

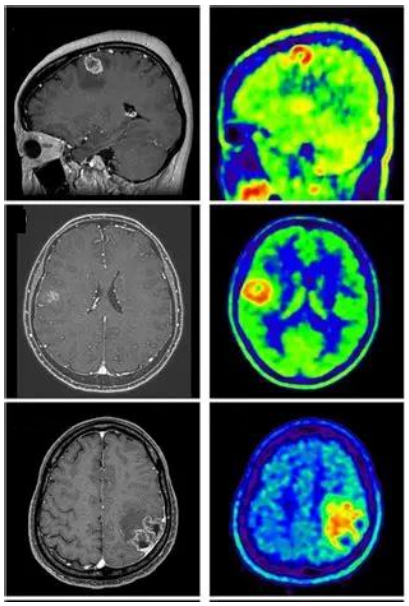

**Figure 7.** MRI to Grad Cam image.

Figure 7 illustrates the transition from the traditional MRI to gradient-weighted class activation for mapping the Grad-CAM. This progression highlights the importance of integrating the visual explanations of the neural networks with the MRI data during the analysis. Figure 8 depicts the distribution of the image ratios.

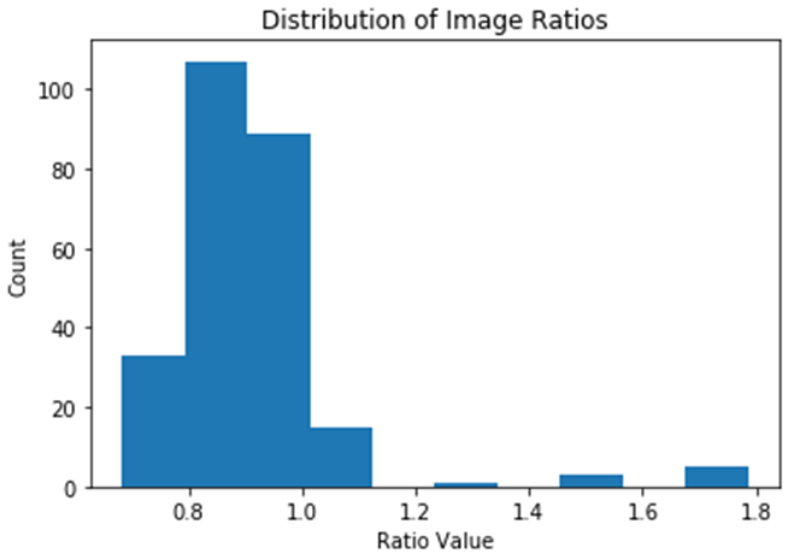


**Figure 8.** Distribution of image ratios.

The Parkinson's Image Dataset shows that most image ratios fall between the range of 0 and 1.2, with 100 occurrences. On the other hand, the number of images in the ratio range of 1.2 to 1.4 has significantly dropped to zero. This indicates that the most images in the dataset have a ratio of less than 1.2, mentioning the vertical orientation rather than horizontal orientation. This understanding of the spread of image proportions can help guide the development of analysis and processing the methods specific to the most common aspect ratios in the dataset.

*4.3. Performance metrics*

1. **Precision**: It is a measure of accuracy for assessing the effectiveness of the model. It calculates the ratio of true positive predictions to all positive predictions made by the model. The precision formula is defined as TP representing correctly predicted positive instances and FP representing incorrectly predicted positive instances, which are shown in equation (9).

$$\text{Precision} = \text{TP} / (\text{TP} + \text{FP}) \tag{9}$$

2. **Recall**: The measure of the model's prediction of actual positive instances. It evaluates how well the model can capture every positive example. The recall formula is represented in equation (10).

$$\text{Recall} = \text{TP} / (\text{TP} + \text{FN}) \tag{10}$$

where FN stands for False Negatives (instances wrongly predicted as negative).

3. **Accuracy:** The accuracy metric assesses how correct the model's predictions are by looking at the percentage of correctly predicted instances, whether positive or negative, out of all instances. Equation (11) signifies the formula of accuracy.

$$\text{Accuracy} = \frac{\text{TP+TN}}{\text{TP+FP+TN+FN}} \tag{11}$$

4. **F1-Score:** The F1-score combines precision and recall into a single metric to evaluate a model's performance, which is particularly effective when there is a disparity in positive and negative instances. It considers precision and recall and offers a unified measurement that demonstrates how well the model performs on predictions for the positive class. The F1-Score formula is calculated as

$$\text{F1-Score} = 2 * (\text{Recall} * \text{Precision}) / (\text{Recall} + \text{Precision}) \quad (12)$$

A higher F1-score signifies improved equilibrium between precision and recall, resulting in superior overall model performance.

### *4.4. Experimental results*

The outcome attained by the projected system is mentioned in this section. Table 1 and Figure 9 illustrate the classification results of the proposed model.

**Table 1.** Classification report of the proposed model.

| Classes | Accuracy | Precision | Recall | F1-Score |
|---|---|---|---|---|
| 0 | 0.98 | 0.95 | 0.96 | 0.98 |
| 1 | 0.98 | 0.93 | 0.97 | 0.96 |

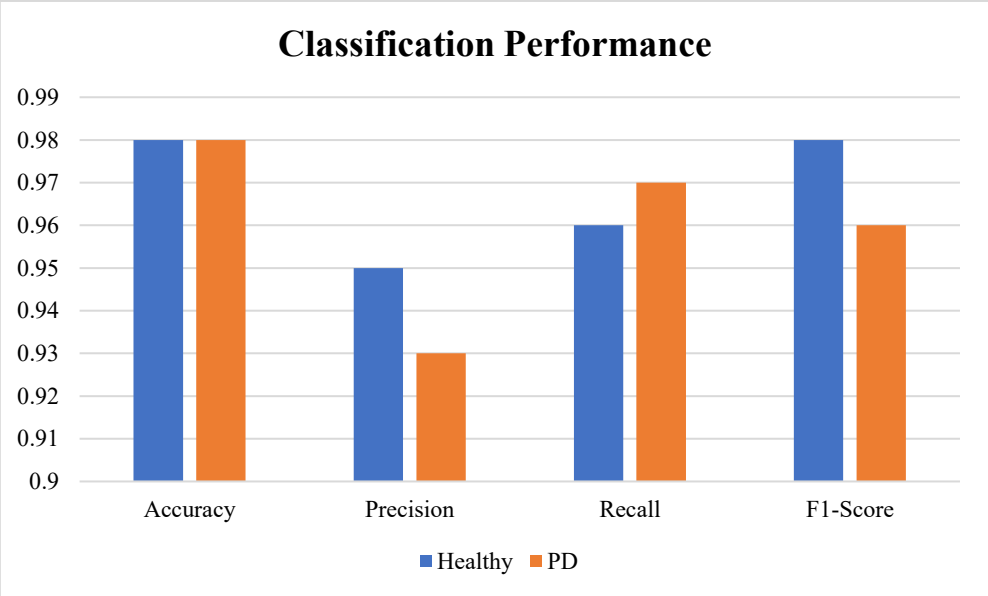


**Figure 9.** Graphical Representation.

The EfficientNet-Feature Sculptor Spatial Net has shown remarkable performance in categorizing the Parkinson's Images Dataset into healthy and PD class 0 (healthy). The precision stands at 95%, a recall of 96%, and the F1-Score at 98%. Likewise, in the case of class 1 (PD), the precision rate stands at 93%, the recall rate at 97%, and the F1-Score at 96%. These measurements show how well the model can accurately differentiate healthy and PD images, confirming its precision with carefully designed layers.

*4.5. Comparative analysis*

This section signifies a comparative analysis of the proposed method with the model. The comparative analysis is performed with internal comparison with classical EfficientNet and external comparison with conventional models. Table 2 and Figure 10 imply the performance analysis of the Traditional and Proposed model.

**Table 2.** Performance Analysis of Traditional and Proposed EfficientNet.

| Methods | Classes | Accuracy | Precision | Recall | F1-Score |
|---|---|---|---|---|---|
| Traditional EfficientNet | 0 | 0.92 | 0.91 | 0.93 | 0.93 |
| | 1 | 0.93 | 0.92 | 0.92 | 0.94 |
| **Proposed EfficientNet** | 0 | 0.98 | 0.95 | 0.96 | 0.98 |
| | 1 | 0.98 | 0.93 | 0.97 | 0.96 |

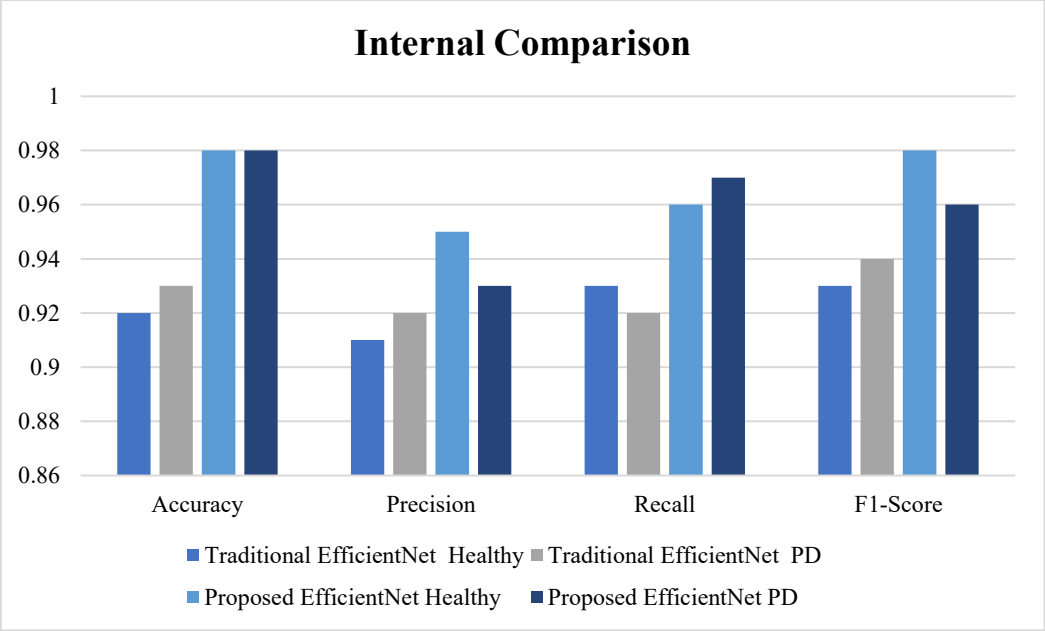


**Figure 10.** Graphical Representation.

The suggested model surpasses the conventional EfficientNet in every aspect. The model performs better for class 0 with higher accuracy (98% vs. 92%), precision (95% vs. 91%), recall (96% vs. 93%), and F1-Score (98% vs. 93%). Likewise, in the case of class 1 (healthy), the suggested model shows better results with increased accuracy (98% compared to 93%), precision (93% compared to 92%), recall (97% compared to 92%), and F1-Score (96% compared to 94%). These findings demonstrate the effectiveness of the suggested model in precisely categorizing Parkinson's images, proving its accuracy with carefully constructed layers. Table 3 and the figure 11 shows a comparative analysis of the projected system with the model.

**Table 3.** Comparative Analysis of Proposed EfficientNet with a Prevailing Method [84].

| Model | Accuracy | Precision | Recall | F1-Score |
|---|---|---|---|---|
| VGG-16 | 0.96 | 0.92 | 0.97 | 0.97 |
| Inception-v3 | 0.78 | 0.75 | 0.71 | 0.73 |
| Resnet-50 | 0.95 | 0.92 | 0.89 | 0.94 |
| Proposed EfficientNet | 0.98 | 0.93 | 0.97 | 0.96 |

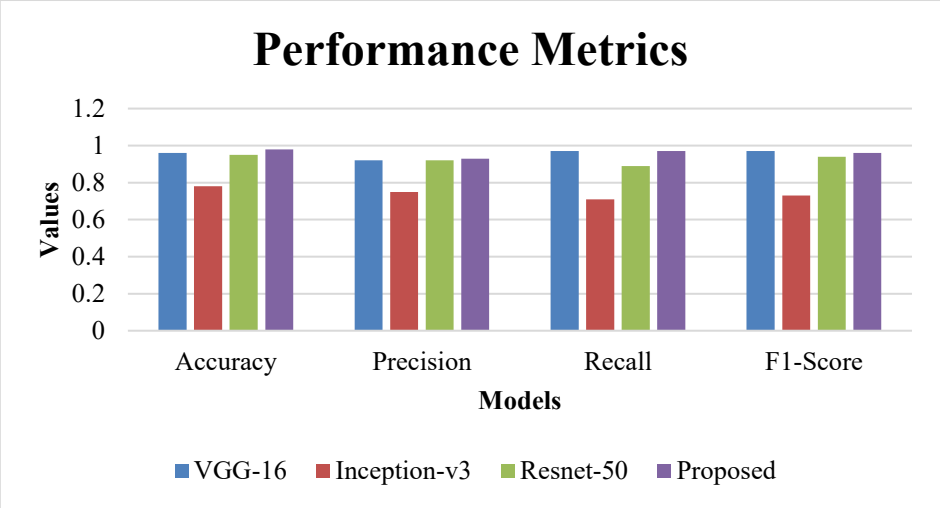


**Figure 11.** Comparative Analysis of the Proposed EfficientNet with the Existing Mechanism [84].

The outcomes show a comparison of different models, such as VGG-16, Inception-v3, ResNet-50, and the suggested model, which were used to classify the Parkinson's Images Dataset into Healthy and PD groups. Of all the models, the suggested model demonstrates the best accuracy (98%). Furthermore, it shows a high level of precision (93%) and recall (97%) by minimizing the errors and accurately capturing the important examples from all the classes. The F1-Score, a combination of precision and recall, is 96%, demonstrating the model's overall success in classifying the Parkinson's images. The results highlight the proposed model's ability and accuracy by demonstrating its potential for an accurate classification. Table 4 and Figure 12 indicate the comparative analysis of the respective system with the pioneering method.

**Table 4.** Comparative Analysis of the Proposed EfficientNet with the Classical System [85].

| Model | Accuracy | Precision | Recall | F1 Score |
|---|---|---|---|---|
| CNN | 0.96 | 0.91 | 0.96 | 0.93 |
| Proposed EfficientNet | 0.98 | 0.93 | 0.97 | 0.96 |

- Comparing the CNN model with the EfficientNet-Feature Sculptor Spatial Net shows notable enhancements in accuracy and precision. The suggested model demonstrates a better performance with an accuracy of 98% compared to the CNN model's 96%. Additionally, the suggested model shows increased accuracy (93% compared to 91%) and the ability to retrieve

the relevant information (97% compared to 96%), leading to a slightly higher combined F1 Score (96% compared to 93%). These findings highlight the success of the suggested model, which was skillfully constructed with carefully planned layers, in precisely classifying Parkinson's images with enhanced accuracy and dependability.

- The model has utilized the Reinforcement Learning Optimization Algorithm (RLOA) to validate its effectiveness on the PPMI dataset and has achieved 98% accuracy compare with the other conventional optimization models. The proposed model has implemented a current State-of-the-Art (SOTA), and the baseline is evaluated on an identical 80:20 PPMI data split. This methodology enables the model to definitively demonstrate the performance benefits resulting from the RLOA architecture by establishing a new and verifiable SOTA.
- Correspondingly, the proposed study has given a unique method using brain scans. Positively, the proposed model is different from other suggested studies that use handwriting and speech samples to look for symptoms like trembling or speech changes.

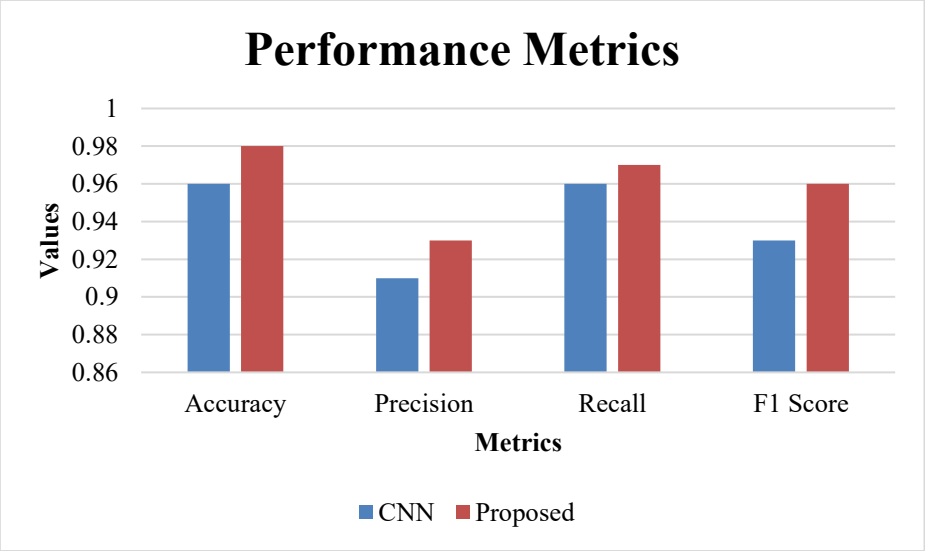


**Figure 12.** Comparative Analysis of the Proposed EfficientNet with the Conventional Approach [85] .

*4.6. Performance analysis*

In this section, we analyze the efficiency of the training set with the test set of the proposed EfficientNet using a confusion matrix and Receiver Operating Characteristic (ROC) curve. The confusion matrix is a fundamental tool in evaluating the performance of classification models. It provides a comprehensive view of a model's prediction accuracy. By analyzing the values, it enables the detection of class imbalances and biases in the model's predictions. Therefore, the overall significance of the confusion matrix offers some insights into the types of errors a model is making. The total sample set utilized for training is 25,000, and the total sample set utilized for testing is about 8,980 samples. The dataset size is 33,980 in total.

Figure 13a shows the confusion matrix of the training set, which correctly identifies 11,429 positive cases (True Positives) and 10,430 negative cases (True Negatives), demonstrating a foundational ability to classify. However, it also misclassifies 2,070 negative cases as positive (False

Positives) and misses 1,071 positive cases, classifying them as negative (False Negatives). This indicates that while the model has a reasonable grasp of the classifications, there is significant room for improvement in reducing both types of errors, as these misclassifications can have perceptible consequences depending on the application.

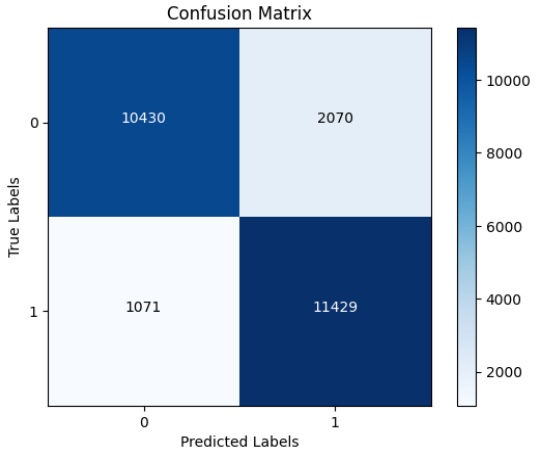


**Figure 13a.** Training Set.

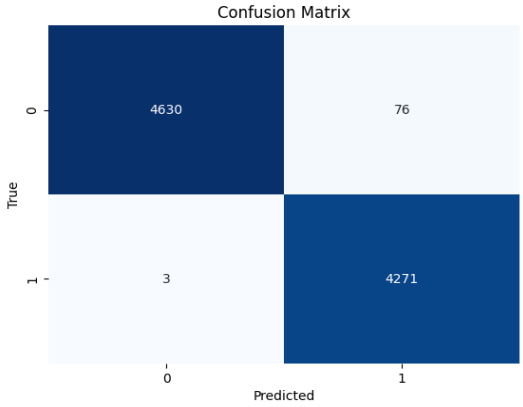


**Figure 13b.** Test Set.

Moreover, the 2nd confusion matrix deliberates the test set, which identifies 4,271 positive cases (True Positives) and 4,630 negative cases (True Negatives), displaying excellent classification prowess. Specifically, it misclassifies only 76 negative cases as positive (False Positives) and misses a mere 3 positive cases, wrongly classifying them as negative (False Negatives). With a low number of both False Positives and False Negatives, a remarkable ability to correctly distinguish positive and negative instances is demonstrated, signifying a robust and reliable model.

Like the confusion matrix, the ROC curve of the proposed and conventional efficient net signifies a graphical representation of a model's diagnostic ability, illustrating the trade-off between the true positive rate (sensitivity) and the false positive rate (1-specificity). This helps assess how well a model distinguishes classes at various threshold values. A higher area under the ROC curve, the Area Under the Curve (AUC), indicates better model performance.

Figure 14 signifies the ROC curve of the proposed and Conventional EfficientNet.

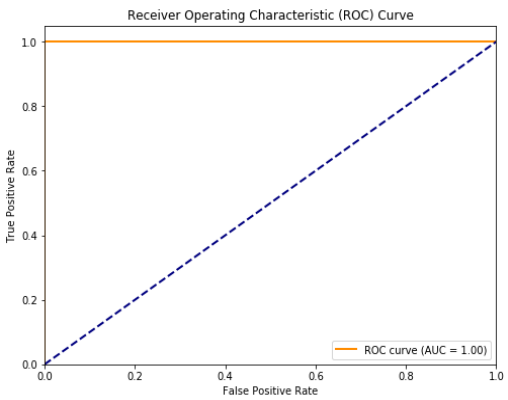


**Figure 14a.** Training set.

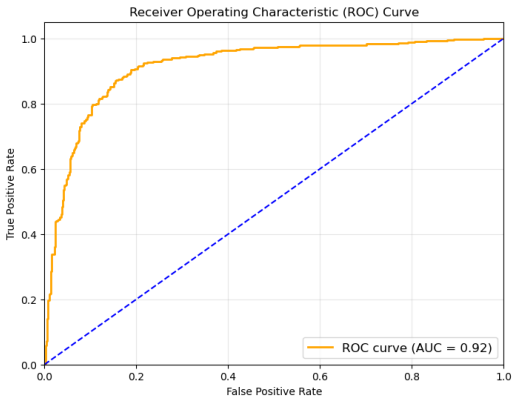


**Figure 14b.** Test set.

In the setting of distinguishing Healthy and PD data for PD, the test set with an AUC value of 0.92 demonstrates better discriminatory power of the classification model. In contrast, the training set exhibits a flawless AUC score of 1.00, a significant accomplishment. The training set consistently achieves slightly higher true positive rates and lower false positive rates across many thresholds compared to the test set. Hence, they accumulate over the curve, resulting in a substantially larger AUC. It effectively distinguishes Healthy and PD categories in the Parkinson's Images Dataset. Its intricate design and detailed layering techniques contribute to its exceptional performance. To prevent data leakage, the strict subject-level split is used and all images from any single subject are confined exclusively to either the training or the testing set. The generalization is further supported by the model's architecture, which uses attention mechanisms to focus on diagnostically relevant features rather than spurious correlations. Additionally, the consistent use of Batch Normalization throughout the network acts as a powerful regulator.

### *4.7. Discussion*

The performance of the EfficientNet-Feature Sculptor Spatial Net model in classifying the Parkinson's Images Dataset into Healthy and PD classes shows an exceptional precision, recall, and F1-Score values, as well as an impressive 98% accuracy for both classes. The model performs well in classifying the normal images with a precision rate of 95%, a recall rate of 96%, and an F1-score of 98% in class 0 (healthy). In the same way, for class 1 (PD), the model demonstrates a precision rate of 93%, a recall rate of 97%, and an F1-Score of 96%. Moreover, the model achieves a higher accuracy, which suggests that the model can make clinical decisions with minimal errors. Moreover, the deployment of the EfficientNet-Feature Sculptor Spatial Net model enables the recognition of complex patterns in medical images that might be difficult for the human eye to detect. Particularly, the model demonstrates high and balanced performance across healthy (Class 0) and PD (Class 1) classes, with high precision, recall, and F1-Scores for both, ensuring that the model is reliable for identifying healthy and diseased states.

The ROC curve of the model shows a perfect AUC value of 1.00, proving its outstanding precision in differentiating healthy and PD categories with no errors. The complex pattern recognition in medical image analysis is made possible by the detailed layering techniques and intricate design of the EfficientNet-Feature Sculptor Spatial Net model, leading to high standards in precision. The benefits and uses of this suggested system reach across fields, such as medical diagnosis, research and development, healthcare automation, telemedicine, drug discovery, and personalized diagnosis. The model's accurate classification abilities can aid in creating custom treatment plans based on each patient's unique characteristics, improving patient results. In general, the suggested EfficientNet-Feature Sculptor Spatial Net model provides a notable improvement in accuracy, precision, and efficiency, with uses in medical diagnosis, research, healthcare automation, telemedicine, drug discovery, and personalized medicine, thereby transforming the realm of medical image analysis.

However, the primary limitation and risk of the proposed EfficientNet-Feature Sculptor Spatial Net with the Reinforcement Learning Optimization Algorithm (RLOA) is that the DRL agent needs several interactions with the neural network to make the training process much longer and more resource-intensive compared to standard models. Additionally, the proposed model is difficult to train and can suffer from instability or convergence issues. Furthermore, a poorly designed reward function could lead the RLOA to an undesirable outcome. Moreover, the proposed model can be subjected to the trade-offs between accuracy and efficiency because the RLOA aims to boost performance by

focusing on relevant data features, which can impact its viability for real-time clinical deployment or use in resource-constrained environments.

Furthermore, the proposed model might have data uncertainties from the data acquisition and pre-processing pipeline. These data-intrinsic and data-processing variations mean that the model's high accuracy might be sensitive to the quality of the incoming raw data stream. Still, the model's reported success relies heavily on specifically tuned parameters for its overall stability and generalizability. Moreover, the proposed model provides a binary classification (Healthy vs. PD) using single-center data. However, there is a need for addressing the differential diagnosis against other neurological conditions, which are needed for the real-world implementation. In future research directions, researchers should focus on validating this promising model using a large-scale, diverse, multi-center dataset. This could provide a visual justification for the model's decisions for the clinicians. Eventually, the model could be prolonged to predict PD severity or progression rates, and its performance could be improved by infusing the image data with other clinical modalities in order to provide a more comprehensive and personalized diagnostic tool.

## 5. Conclusions

PD is a brain disorder with wide variability in severity among individuals. Detecting the disease promptly is essential to prevent potential negative outcomes later on. Identifying PD manually is a slow process with low effectiveness and is susceptible to human mistakes. Traditional studies used AI technology to automate the classification of PD to address the problem. Nevertheless, traditional systems encounter problems such as precision, data over-fitting, and managing big datasets. To address this, the proposed model employs the EfficientNet System with a focus on refining features through layers of the Spatial Net. EfficientNet is utilized for its benefits in terms of improved parameter efficiency, computational tradeoff, and better regularization techniques, among others. On the other hand, it falls short in terms of efficacy, complexity, understanding of internal representation, and more. In response to this challenge, the proposed system incorporates Feature Sculptor Spatial Net to enhance classification efficiency through precision crafting across layers. Certain performance metrics are used to calculate the performance of the predicted model. The results show that the research achieves high precision, recall, and F1-score values with 98% accuracy for both classes. In the standard class (class 0), the precision rate is 95%, the recall rate is 96%, and the F1-Score is 98%. Similarly, for class 1 (healthy), the precision rate is 93%, the recall rate is 97%, and the F1-Score is 96%. These measurements indicate the model's ability to accurately distinguish Healthy and PD images, validating its precision through thoughtfully constructed layers. Though this study results in effective outcomes, we focus only on binary classification; however, multi-classification can be explored in the future. Additionally, integrating real-time analytics, such as mobile apps, could provide timely monitoring and personalized interventions, further advancing the management of PD.

## Use of AI tools declaration

The author(s) declare(s) they have used Artificial Intelligence (AI) tools in the creation of this article.

## Conflict of interest

The author reports that there is no conflict of interest.

## Ethical statement for human participants

All patient data is de-identified with prior informed consent, adhering to the PPMI's ethical guidelines.

## References


1. R. Bhidayasiri, J. Sringean, S. Phumphid, C. Anan, C. Thanawattano, S. Deoisres, et al., The rise of Parkinson's disease is a global challenge, but efforts to tackle this must begin at a national level: A protocol for national digital screening and 'eat, move, sleep' lifestyle interventions to prevent or slow the rise of non-communicable diseases in Thailand, *Front. Neurol.,* **15** (2024), 1386608. https://doi.org/10.3389/fneur.2024.1386608
2. P. Vitali, M. I. Pan, F. Palesi, G. Germani, A. Faggioli, N. Anzalone, et al., Substantia Nigra volumetry with 3-T MRI in De novo and advanced Parkinson disease, *Radiology,* **296** (2020), 401–410. https://doi.org/10.1148/radiol.2020191235
3. Y. Zhao, P. Wu, J. Wu, M. Brendel, J. Lu, J. Ge, et al., Decoding the dopamine transporter imaging for the differential diagnosis of parkinsonism using deep learning, *Eur. J. Nucl. Med. Mol. Imaging*, **49** (2022), 2798–2811. https://doi.org/10.1007/s00259-022-05804-x
4. Y. Ben-Shlomo, S. Darweesh, J. Llibre-Guerra, C. Marras, M. San Luciano, C. Tanner, The epidemiology of Parkinson's disease, *Lancet*, **403** (2024), 283–292. https://doi.org/10.1016/S0140-6736(23)01419-8
5. A. Radlicka-Borysewska, J. Jabłońska, M. Lenarczyk, Ł. Szumiec, Z. Harda, M. Bagińska, et al., Non-motor symptoms associated with progressive loss of dopaminergic neurons in a mouse model of Parkinson's disease, *Front. Neurosci.*, **18** (2024), 1375265. https://doi.org/10.3389/fnins.2024.1375265
6. W. G. Meissner, P. Remy, C. Giordana, D. Maltête, P. Derkinderen, J.-L. Houéto, et al., Trial of Lixisenatide in early Parkinson's disease, *N. Engl. J. Med.*, **390** (2024), 1176–1185. https://doi.org/10.1056/NEJMoa2312323
7. X. Cao, F. Yang, J. Zheng, X. Wang, Q. Huang, Aberrant structure MRI in Parkinson's disease and comorbidity with depression based on multinomial tensor regression analysis, *J. Pers. Med.,* **12** (2022), 89. https://doi.org/10.3390/jpm12010089
8. A. Boutet, R. Madhavan, G. J. Elias, S. E. Joel, R. Gramer, M. Ranjan, et al., Predicting optimal deep brain stimulation parameters for Parkinson's disease using functional MRI and machine learning, *Nat. Commun.*, **12** (2021), 3043. https://doi.org/10.1038/s41467-021-23311-9
9. E. Porter, A.-A. Roussakis, N.P. Lao-Kaim, P. Piccini, Multimodal dopamine transporter (DAT) imaging and magnetic resonance imaging (MRI) to characterise early Parkinson's disease, *Parkinson. Relat. Disord.,* **79** (2020), 26–33. https://doi.org/10.1016/j.parkreldis.2020.08.010
10. N. He, Y. Chen, P. A. LeWitt, F. Yan, E. M. Haacke, Application of neuromelanin MR imaging in Parkinson disease, *J. Magn. Reson. Imaging,* **57** (2023), 337–352. https://doi.org/10.1002/jmri.28414
11. E. Düzel, M. Costagli, G. Donatelli, O. Speck, M. Cosottini, Studying Alzheimer disease,

Parkinson disease, and amyotrophic lateral sclerosis with 7-T magnetic resonance, *Eur. Radiol. Exp.,* **5** (2021), 1–17. https://doi.org/10.1186/s41747-021-00221-5

12. G. P. A. Mary, N. Suganthi, M. Hema, Early prediction of Parkinson's disease from brain MRI images using Convolutional Neural Network, *J. Med. Imaging Health Inform.,* **11** (2021), 3103–3109. https://doi.org/10.1166/jmihi.2021.3897
13. L. Chougar, A. Faucher, J. Faouzi, F. X. Lejeune, G. G. Lobo, C. Jovanovic, et al., Contribution of MRI for the early diagnosis of parkinsonism in patients with diagnostic uncertainty, *Mov. Disord,* (2024). https://doi.org/10.1002/mds.29760
14. H. C. Moon, A. Kim, Y. S. Park, Brain structure comparison among Parkinson disease, essential tremor, and healthy controls using 7T MRI, *Medicine,* **103** (2024), e38139. https://doi.org/10.1097/MD.0000000000038139
15. M. Ariz, M. Martínez, I. Alvarez, M. A. Fernández-Seara, G. Castellanos, C. N. P. S. D. Consortium, et al., Automatic segmentation and quantification of Nigrosome-1 neuromelanin and iron in MRI: A candidate biomarker for Parkinson's disease, *J. Magn. Reson. Imaging,* (2023). https://doi.org/10.1002/jmri.29073
16. R. Martins, F. Oliveira, F. Moreira, A. P. Moreira, A. Abrunhosa, C. Januário, et al., Automatic classification of idiopathic Parkinson's disease and atypical Parkinsonian syndromes combining [11C] raclopride PET uptake and MRI grey matter morphometry, *J. Neural Eng.,* **18** (2021), 046037. https://doi.org/10.1088/1741-2552/abf772
17. K. P. Nguyen, V. Raval, A. Treacher, C. Mellema, F. F. Yu, M. C. Pinho, et al., Predicting Parkinson's disease trajectory using clinical and neuroimaging baseline measures. *Parkinson. Relat. Disord.,* **85** (2021), 44–51. https://doi.org/10.1016/j.parkreldis.2021.02.026
18. M. Arafe, N. Bhagwat, Y. Chatelain, M. Dugré, A. Sokołowski, M. Wang, et al., Predicting Parkinson's disease progression using MRI-based white matter radiomic biomarker and machine learning: A reproducibility and replicability study, *bioRxiv*, (2023), 2023.05. 05.539590. Available from: https://www.biorxiv.org/content/10.1101/2023.05.05.539590.abstract
19. S. G. Ryman, K. L. Poston, MRI biomarkers of motor and non-motor symptoms in Parkinson's disease, *Parkinson. Relat. Disord.,* **73** (2020), 85–93. https://doi.org/10.1016/j.parkreldis.2019.10.002
20. N. Xu, Y. Zhou, A. Patel, N. Zhang, Y. Liu, Parkinson's disease diagnosis beyond clinical features: A bio-marker using topological machine learning of resting-state functional magnetic resonance imaging, *Neuroscience,* **509** (2023), 43–50. https://doi.org/10.1016/j.neuroscience.2022.11.022
21. G. Solana-Lavalle, R. Rosas-Romero, Classification of PPMI MRI scans with voxel-based morphometry and machine learning to assist in the diagnosis of Parkinson's disease, *Comput. Methods Programs Biomed.,* **198** (2021), 105793. https://doi.org/10.1016/j.cmpb.2020.105793
22. V. Muñoz-Ramírez, V. Kmetzsch, F. Forbes, S. Meoni, E. Moro, M. Dojat, Subtle anomaly detection in MRI brain scans: Application to biomarkers extraction in patients with de novo Parkinson's disease, medRxiv, (2021), 2021.06. 03.21258269. https://doi.org/10.1101/2021.06.03.21258269
23. C. Song, W. Zhao, H. Jiang, X. Liu, Y. Duan, X. Yu, et al., Stability evaluation of brain changes in Parkinson's disease based on machine learning, *Front. Comput. Neurosci.*, **15** (2021), 735991. https://doi.org/10.3389/fncom.2021.735991
24. J. Prasuhn, M. Heldmann, T. F. Münte, N. Brüggemann, A machine learning-based classification approach on Parkinson's disease diffusion tensor imaging datasets, *Neurol. Res. Pract.,* **2** (2020),

1–5. https://doi.org/10.1186/s42466-020-00092-y
25. N. Radha, R. S. Madhavan, Parkinson's disease detection using machine learning techniques, *Int. J. Early Child. Spec. Educ.,* **30** (2021), 543. https://doi.org//10.24205/03276716.2020.4055
26. S. Chakraborty, S. Aich, H.-C. Kim, 3D textural, morphological and statistical analysis of voxel of interests in 3T MRI scans for the detection of Parkinson's disease using artificial neural networks, *Healthcare*, (2020), 34.
27. I. El Maachi, G.-A. Bilodeau, W. Bouachir, Deep 1D-Convnet for accurate Parkinson disease detection and severity prediction from gait, *Expert Syst. Appl,* **143** (2020), 113075. https://doi.org/10.1016/j.eswa.2019.113075
28. S. Kanagaraj, M. Hema, M. N. Guptha, An improved approach for early diagnosis of Parkinson's disease using advanced DL models and image alignment, *Automatika,* **65** (2024), 911–924. https://doi.org/10.1080/00051144.2023.2284030
29. M. A. Al-Khasawneh, A. Alzahrani, A. Alarood, An artificial intelligence based effective diagnosis of Parkinson disease using EEG signal, data analysis for neurodegenerative disorders, Springer, 2023, pp. 239–251.
30. M. Alrawis, S. Al-Ahmadi, F. Mohammad, Bridging modalities: A multimodal machine learning approach for Parkinson's disease diagnosis using EEG and MRI data, *Appl. Sci.,* **14** (2024), 3883. https://doi.org/10.3390/app14093883
31. Y. Huang, K. Chaturvedi, A.-A. Nayan, M. H. Hesamian, A. Braytee, M. Prasad, Early Parkinson's disease diagnosis through hand-drawn spiral and wave analysis using deep learning techniques, *Information,* **15** (2024), 220. https://doi.org/10.3390/info15040220
32. N. Chintalapudi, G. Battineni, M. A. Hossain, F. Amenta, Cascaded deep learning frameworks in contribution to the detection of parkinson's disease, *Bioengineering,* **9** (2022), 116. https://doi.org/10.3390/bioengineering9030116
33. Y. Chen, G. Zhu, D. Liu, Y. Liu, T. Yuan, X. Zhang, et al., Brain morphological changes in hypokinetic dysarthria of Parkinson's disease and use of machine learning to predict severity, *CNS Neurosci. Ther,* **26** (2020), 711–719. https://doi.org/10.1111/cns.13304
34. K. H. Leung, S. P. Rowe, M. G. Pomper, Y. Du, A three-stage, deep learning, ensemble approach for prognosis in patients with Parkinson's disease, *EJNMMI Res.,* **11** (2021), 1–14. https://doi.org/10.1186/s13550-021-00795-6
35. A. A. Nguyen, P. D. Maia, X. Gao, P. F. Damasceno, A. Raj, Dynamical role of pivotal brain regions in Parkinson symptomatology uncovered with deep learning, *Brain Sci.,* **10** (2020), 73. https://doi.org/10.3390/brainsci10020073
36. R. Jyothika, D. C. Bhavyasri, Parkinson disease detection using deep CNN model, *Turk. J. Comput. Math. Educ.,* **14** (2023), 675–683.
37. S. Chakraborty, S. Aich, H.-C. Kim, Detection of Parkinson's disease from 3T T1 weighted MRI scans using 3D convolutional neural network, *Diagnostics,* **10** (2020), 402. https://doi.org/10.3390/diagnostics10060402
38. S. Yadav, Bayesian deep learning based convolutional neural network for classification of Parkinson's disease using functional magnetic resonance images, (2021). Available from: https://papers.ssrn.com/sol3/papers.cfm?abstract_id=3833760
39. M. Nour, U. Senturk, K. Polat, Diagnosis and classification of Parkinson's disease using ensemble learning and 1D-PDCovNN, *Comput. Biol. Med.,* **161** (2023) 107031. https://doi.org/10.1016/j.compbiomed.2023.107031

40. R. Gaurav, R. Valabrègue, L. Yahia-Chérif, G. Mangone, S. Narayanan, I. Arnulf, et al., NigraNet: An automatic framework to assess nigral neuromelanin content in early Parkinson's disease using convolutional neural network, *Neuroimage Clin.,* **36** (2022), 103250. https://doi.org/10.1016/j.nicl.2022.103250
41. H. Zhao, C.-C. Tsai, M. Zhou, Y. Liu, Y.-L. Chen, F. Huang, et al., Deep learning based diagnosis of Parkinson's disease using diffusion magnetic resonance imaging, *Brain Imaging Behav.,* **16** (2022), 1749–1760. https://doi.org/10.1007/s11682-022-00631-y
42. E. Huseyn, Deep learning based early diagnostics of Parkinsons disease, arXiv preprint, (2020), arXiv:2008.01792. https://doi.org/10.48550/arXiv.2008.01792
43. A.G. Mohammadi, P. Mehralian, A. Naseri, H. Sajedi, Parkinson's disease diagnosis: The effect of autoencoders on extracting features from vocal characteristics, *Array*, **11** (2021), 100079. https://doi.org/10.1016/j.array.2021.100079
44. Y. Ya, L. Ji, Y. Jia, N. Zou, Z. Jiang, H. Yin, et al., Machine learning models for diagnosis of parkinson's disease using multiple structural magnetic resonance imaging features, *Front. Aging Neurosci.,* **14** (2022), 808520. https://doi.org/10.3389/fnagi.2022.808520
45. H. Shibata, Y. Uchida, S. Inui, H. Kan, K. Sakurai, N. Oishi, et al., Machine learning trained with quantitative susceptibility mapping to detect mild cognitive impairment in Parkinson's disease, *Parkinson. Relat. Disord.,* **94** (2022), 104–110. https://doi.org/10.1016/j.parkreldis.2021.12.004
46. R. Ranjbarzadeh, A. Keles, M. Crane, M. Bendechache, Comparative analysis of real-clinical MRI and BraTS datasets for brain tumor segmentation, CP887, *IET*, (2024), pp. 39–46.
47. A. Naseer, M. Rani, S. Naz, M.I. Razzak, M. Imran, G. Xu, Refining Parkinson's neurological disorder identification through deep transfer learning, *Neural Comput. Appl.,* (2020). https://doi.org/10.1007/s00521-019-04069-0
48. S. Suchitra, Parkinson disease prediction using deep learning algorithm, rp-9788770040723.217.
49. P. Wu, Y. Zhao, J. Wu, M. Brendel, J. Lu, J. Ge, et al., Differential diagnosis of parkinsonism based on deep metabolic imaging indices, *J. Nucl. Med.,* **63** (2022), 1741–1747. https://doi.org/10.2967/jnumed.121.263029
50. L. Nanni, M. Interlenghi, S. Brahnam, C. Salvatore, S. Papa, R. Nemni, et al., Comparison of transfer learning and conventional machine learning applied to structural brain MRI for the early diagnosis and prognosis of Alzheimer's disease, *Front. Neurol.,* **11** (2020), 576194. https://doi.org/10.3389/fneur.2020.576194
51. S. Sivaranjini, C. Sujatha, Deep learning based diagnosis of Parkinson's disease using convolutional neural network, *Multimed. Tools Appl.,* **79** (2020), 15467–15479. https://doi.org/10.1007/s11042-019-7469-8
52. D. Yin, Y. Zhao, Y. Wang, W. Zhao, X. Hu, Auxiliary diagnosis of heterogeneous data of Parkinson's disease based on improved convolution neural network. *Multimed. Tools Appl.,* **79** (2020), 24199–24224. https://doi.org/10.1007/s11042-020-08984-6
53. C. Zhou, L. Wang, W. Cheng, J. Lv, X. Guan, T. Guo, et al., Two distinct trajectories of clinical and neurodegeneration events in Parkinson's disease. *NPJ Parkinson's Disease,* **9** (2023), 111. https://doi.org/10.1038/s41531-023-00556-3
54. T. Vyas, R. Yadav, C. Solanki, R. Darji, S. Desai, S. Tanwar, Deep learning-based scheme to diagnose Parkinson's disease, *Expert Syst.,* **39** (2022), e12739. https://doi.org/10.1111/exsy.12739
55. R. Ranjbarzadeh, A. Caputo, E. B. Tirkolaee, S. J. Ghoushchi, M. Bendechache, Brain tumor segmentation of MRI images: A comprehensive review on the application of artificial intelligence

tools, *Comput. Biol. Med.,* **152** (2023), 106405. https://doi.org/10.1016/j.compbiomed.2022.106405
56. T. Varrecchia, S. F. Castiglia, A. Ranavolo, C. Conte, A. Tatarelli, G. Coppola, et al., An artificial neural network approach to detect presence and severity of Parkinson's disease via gait parameters, *PLoS One,* **16** (2021), e0244396. https://doi.org/10.1371/journal.pone.0244396
57. B. Anusha, P. Geetha, A. Kannan, Parkinson's disease identification in homo sapiens based on hybrid ResNet-SVM and resnet-fuzzy svm models, *J. Intell. Fuzzy Syst.,* **43** (2022), 2711–2729. https://doi.org/10.3233/JIFS-220271
58. H. Kuresan, D. Samiappan, A. Jeevan, S. Gupta, Performance study of ML models and neural networks for detection of Parkinson disease using dysarthria symptoms, *Eur. J. Mol. Clin. Med.,* **8** (2021), 767–779. Available from: https://d1wqtxts1xzle7.cloudfront.net/80116003/article_9520_1054f2d0625eb6b99aab15d372387b36-libre.pdf
59. Z. K. Senturk, Early diagnosis of Parkinson's disease using machine learning algorithms, *Med. Hypoth.,* **138** (2020), 109603. https://doi.org/10.1016/j.mehy.2020.109603
60. A. Mozhdehfarahbakhsh, S. Chitsazian, P. Chakrabarti, T. Chakrabarti, B. Kateb, M. Nami, An MRI-based deep learning model to predict Parkinson's disease stages, medRxiv (2021), 2021.02.19.21252081. https://doi.org/10.1101/2021.02.19.21252081
61. N. T. Sarshar, S. Sadeghi, M. Kamsari, M. Avazpour, S. J. Ghoushchi, R. Ranjbarzadeh, Advancing brain MRI images classification: Integrating VGG16 and ResNet50 with a Multi-verse optimization method, (2024).
62. R. Ranjbarzadeh, A. B. Kasgari, S. J. Ghoushchi, S. Anari, M. Naseri, M. Bendechache, Brain tumor segmentation based on deep learning and an attention mechanism using MRI multi-modalities brain images, *Sci. Rep.*, **11** (2021), 10930. https://doi.org/10.1038/s41598-021-90428-8
63. E. Moya-Sáez, Ó. Peña-Nogales, R. de Luis-García, C. Alberola-López, A deep learning approach for synthetic MRI based on two routine sequences and training with synthetic data, *Comput. Methods Programs Biomed.,* **210** (2021), 106371. https://doi.org/10.1016/j.cmpb.2021.106371
64. G. Pahuja, B. Prasad, Deep learning architectures for Parkinson's disease detection by using multi-modal features, *Comput. Biol. Med.,* **146** (2022), 105610. https://doi.org/10.1016/j.compbiomed.2022.105610
65. X. Guo, S. Tinaz, N. C. Dvornek, Characterization of early stage Parkinson's disease from resting-state fMRI data using a long short-term memory network, *Front. Neuroimag.,* **1** (2022), 952084. https://doi.org/10.3389/fnimg.2022.952084
66. J. Zhang, Mining imaging and clinical data with machine learning approaches for the diagnosis and early detection of Parkinson's disease, *NPJ Parkinson's Disease,* **8** (2022) 13. https://doi.org/10.1038/s41531-021-00266-8
67. E. Balaji, D. Brindha, V.K. Elumalai, R. Vikrama, Automatic and non-invasive Parkinson's disease diagnosis and severity rating using LSTM network, *Appl. Soft Comput.,* **108** (2021) 107463. https://doi.org/10.1016/j.asoc.2021.107463
68. A. B. Kasgari, R. Ranjbarzadeh, A. Caputo, S. B. Saadi, M. Bendechache, Brain tumor segmentation based on zernike moments, enhanced ant lion optimization, and convolutional neural network in MRI images, in: *Metaheuristics and Optimization in Computer and Electrical Engineering*, *Hybrid and Improved Algorithms*, Springer, **2** (2023), pp. 345–366.
69. K. Santhosh, P. P. Dev, Z. Lynton, P. Das, E. Ghaderpour, A modified Gray Wolf optimization

algorithm for early detection of Parkinson's disease, *Biomed. Signal Process. Control,* **109** (2025), 108061. https://doi.org/10.1016/j.bspc.2025.108061

70. M. A. Islam, M. Z. H. Majumder, M. A. Hussein, K. M. Hossain, M. S. Miah, A review of machine learning and deep learning algorithms for Parkinson's disease detection using handwriting and voice datasets, *Heliyon*, **10** (2024). Available from: https://www.cell.com/heliyon/fulltext/S2405-8440(24)01500-7
71. L. Su, K. A. Alattas, W. Ayadi, Z. Lynton, E. Ghaderpour, A. Mohammadzadeh, et al., A novel fuzzy reinforcement learning approach for personalization deep brain stimulation with communication delay, *Biomed. Signal Process. Control*, **106** (2025), 107736. https://doi.org/10.1016/j.bspc.2025.107736
72. S. Kaur, H. Aggarwal, R. Rani, Diagnosis of Parkinson's disease using deep CNN with transfer learning and data augmentation, *Multimed. Tools Appl.,* **80** (2021), 10113–10139. https://doi.org/10.1007/s11042-020-10114-1
73. R. Ranjbarzadeh, M. Crane, M. Bendechache, The impact of backbone selection in Yolov8 Models on brain tumor localization, *Iran J. Comput. Sci.,* (2025), 1–23. https://doi.org/10.1007/s42044-025-00258-4
74. W. Wang, J. Lee, F. Harrou, Y. Sun, Early detection of Parkinson's disease using deep learning and machine learning, *IEEE Access,* **8** (2020), 147635–147646. https://doi.org/10.1109/ACCESS.2020.3016062
75. R. Ranjbarzadeh, A. Keles, M. Crane, S. Anari, M. Bendechache, Secure and decentralized collaboration in oncology: A blockchain approach to tumor segmentation, *IEEE*, 2024, pp.1681–1686.
76. M. O. Etekochay, A. R. Amaravadhi, G. V. González, A. G. Atanasov, M. Matin, M. Mofatteh, et al., Unveiling new strategies facilitating the implementation of artificial intelligence in neuroimaging for the early detection of Alzheimer's disease, *J. Alzheimers Dis.,* **99** (2024), 1–20. https://doi.org/10.3233/JAD-231135
77. S. Bajaj, M. Khunte, N. S. Moily, S. Payabvash, M. Wintermark, D. Gandhi, et al., Value proposition of FDA-approved artificial intelligence algorithms for neuroimaging, *J. Am. Coll. Radiol.,* **20** (2023), 1241–1249. https://doi.org/10.1016/j.jacr.2023.06.034
78. S. Rajaraman, Artificial intelligence in Neuro degenerative diseases: Opportunities and challenges, *AI Neuro-Degener. Diseases Insights Solut.*, (2024), 133–153. https://doi.org/10.1007/978-3-031-53148-4_8
79. N. Hastings, D. Samuel, A. N. Ansari, P. Kaurani, V. S. Bhandary, P. Gautam, et al., The role of artificial intelligence-powered imaging in cerebrovascular accident detection, *Cureus*, **16** (2024). https://doi.org/10.7759/cureus.59768
80. T. Robertson, D. Taylor, C. Taylor, J. Patterson, Utilization of artificial intelligence to improve door-in door-out times for mechanical thrombectomy-eligible patients at a hub-and-spoke community-based comprehensive stroke center: A single case study presentation: AI improving DIDO times, *Stroke Clin.,* (2024). https://journals.psu.edu/strokeclinician/article/view/53
81. M. Amin, E. Martínez-Heras, D. Ontaneda, F. P. Carrasco, Artificial intelligence and multiple sclerosis, *Curr. Neurol. Neurosci. Rep,* **24** (2024), 233–243. https://doi.org/10.1007/s11910-024-01354-x
82. A. Di Ieva, Fractals, pattern recognition, memetics, and AI: A personal journal in the computational neurosurgery, *Springer*, 2024, pp. 273–283.

83. P. Vedmurthy, A. L. Pinto, D. D. Lin, A. M. Comi, Y. Ou, Study protocol: Retrospectively mining multisite clinical data to presymptomatically predict seizure onset for individual patients with Sturge-Weber, *BMJ Open*, **12** (2022), e053103. Available from: https://bmjopen.bmj.com/content/12/2/e053103.abstract
84. C. Srinivas, N. P. KS, M. Zakariah, Y. A. Alothaibi, K. Shaukat, B. Partibane, et al., Deep transfer learning approaches in performance analysis of brain tumor classification using MRI images, *J. Healthc. Eng.,* **2022** (2022). https://doi.org/10.1155/2022/3264367
85. M. Islam, M. T. Reza, M. Kaosar, M. Z. Parvez, Effectiveness of federated learning and CNN ensemble architectures for identifying brain tumors using MRI images, *Neural Process. Lett.,* **55** (2023), 3779–3809. https://doi.org/10.1007/s11063-022-11014-1


AIMS Press